Metallic properties of Li-intercalated carbon nanotubes investigated by NMR

M. Schmid,[1,2,3] C. Goze-Bac,[1,*] S. Krämer,[2,4] S. Roth,[3] M. Mehring,[2] C. Mathis,[5] and P. Petit[5]
[1]*LCVN, CNRS-Université Montpellier 2, France*
[2]*Physikalisches Institut, Universität Stuttgart, Pfaffenwaldring 57, D-70550 Stuttgart, Germany*
[3]*Max-Planck-Institut für Festkörperforschung, Heisenbergstrasse 1, D-70569 Stuttgart, Germany*
[4]*CNRS–Laboratoire des Champs Magnétiques Intenses, 25 avenue des Martyrs, 38042 Grenoble Cedex 9, France*
[5]*Institut Charles Sadron, 6 rue Boussingault, 67000 Strasbourg Cedex, France*
(Received 22 February 2006; published 31 August 2006)

Electronic properties of single-walled carbon nanotubes intercalated with lithium are investigated by NMR. ^{13}C NMR experiments reveal a metallic ground state for all of the following stoichiometries LiC_x with $x=10$, 7, and 6. A continuous increase of the density of states at the Fermi level according to the Li concentration is observed up to $x\approx 6$. From ^{7}Li NMR, evidence of inequivalent Li sites is reported, corresponding to preferential sites of intercalation and binding between Li and C.

DOI: 10.1103/PhysRevB.74.073416 PACS number(s): 81.07.De, 73.22.−f, 82.56.−b

Since the invention of lithium-ions batteries, carbon-based materials such as natural graphite, carbon fibers, and pyrolitic carbon were proposed as possible candidates for the use as battery anode materials.[1] Recently, new progress has been reported in the use of single-walled carbon nanotubes (SWNTs) for this purpose.[2] At the same time, it has been shown that a new class of synthetic metals based on alkali intercalated nanotubes can be synthesized.[3–5] Because of their one-dimensional electronic structure and high tensile strength,[6] these one-dimensional metals are promising materials. A large variety of solid-state properties has been reported ranging from insulator to metal and superconductor. However, all potential applications these materials offer depend strongly on the structures, compositions, and stoichiometries. We report on chemically Li-intercalated SWNT at different concentrations using high-resolution NMR techniques. We show how the alkali content controls the electronic properties of the metallic ground state and clarify the structural and dynamical properties of Li.

SWNT samples used in this study were synthesized by the electric arc method under the conditions described in Refs. 7 and 8. In order to improve the ^{13}C NMR signal-to-noise ratio, 10% ^{13}C isotope enriched graphitic rods were vaporized in the presence of a catalyst mixture in the molar proportions 96.8% C, 2.1% Rh, and 1.1% Pt. The SWNT bundles were collected directly from the collerette and used as produced without any purification. We estimated a content of over 80% carbon nanotubes showing an average diameter of 1.4 nm and a bundle length of several micrometers (see Refs. 8 and 9 for more details about the samples). Lithium was chemically intercalated in SWNT ropes by using solutions of aromatic hydrocarbons and tetrahydrofuran (THF). By redox reactions between the radical anions of fluorenone, benzophenone, naphthalene, and SWNT with Li^+ as a counter ion, intercalated SWNTs were synthesized with stoichiometries of LiC_{10}, LiC_7, and LiC_6, respectively.[10] All samples were sealed under high vacuum. The experimental sample preparation conditions as well as a detailed Raman characterization are described elsewhere.[10–12] It has been shown that an electronic charge transfer occurs from the aromatic hydrocarbons to the SWNT bundles. Similarly to the intercalation process in other carbon materials, the alkali are expected to be intercalated together with THF molecules used as a solvent, forming a ternary compound $Li(THF)_yC_x$.[13–15]

^{13}C NMR experiments were carried out on a Bruker ASX200 spectrometer at a magnetic field of 4.7 T and a Larmor frequency of 50.3 MHz. High-resolution ^{13}C NMR at magic angle spinning (MAS) was performed at room temperature with spinning frequencies from 4 up to 9 kHz. ^{13}C NMR static spectra were obtained in the temperature range of 50–300 K. ^{7}Li NMR measurements were performed on a homebuilt pulsed NMR spectrometer equipped with a sweep magnet working at 4.2 and 6 T corresponding to Larmor frequencies of 70.2 and 100 MHz, respectively. ^{13}C NMR line shifts were referred to TMS and ^{7}Li NMR line shifts to 1 M LiCl as an external standard. Spin lattice relaxation rates $1/T_1$ were obtained using a saturation recovery pulse technique and a Hahn echo as a detection sequence.

Static and high-resolution MAS ^{13}C NMR spectra of the pristine and Li-intercalated SWNT are presented in Fig. 1. The static spectra on the left side show the evolution of the

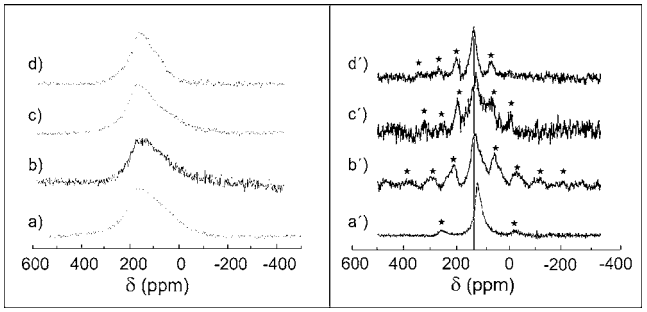

FIG. 1. ^{13}C NMR spectra ($\omega_0=50.3$ MHz) at room temperature of pristine SWNT (Ref. 9) (a) and LiC_x intercalated compounds with $x=10$, 7, and 6 [(b), (c), and (d), respectively]. On the left side, the static ^{13}C NMR spectra are presented and on the right side the high-resolution ^{13}C MAS NMR spectra. The symbols ⋆ are for the spinning sidebands. Spinning rates are about 9 kHz in (a′) and 4 kHz in (b′), (c′), and (d′).

sp^2 powder pattern line shape of SWNTs under Li intercalation. A clear anisotropy reduction of about 200 ppm is observed with increasing content of intercalated Li from LiC_{10} to LiC_6. The sideband distributions of the corresponding MAS spectra on the right side of Fig. 1 confirm this fact. In addition, the isotropic line positions δ_{iso} are paramagnetically shifted from 126 ppm for pristine SWNT (Refs. 8 and 9) up to 136 ppm in LiC_6. According to the literature on carbon intercalation compounds,[16,17] these observations indicate important modifications of the electronic properties and suggest that all samples exhibit a metallic state tunable by the amount of intercalated Li.

In order to interpret our data, we developed the following analysis. The observed shift $\boldsymbol{\delta}$ can be separated into two parts, the chemical shift $\boldsymbol{\sigma}$ and the Knight shift $\mathbf{K}$, according to

$$\boldsymbol{\delta} = \boldsymbol{\sigma} + \mathbf{K}, \tag{1}$$

where $\boldsymbol{\sigma}$ and $\mathbf{K}$ are second-rank tensors consisting of an isotropic and an anisotropic part. The chemical shift $\boldsymbol{\sigma}$ arises from local orbital magnetic fields caused by local currents in the sample. The Knight shift $\mathbf{K}$ arises from the hyperfine coupling of conduction electron spins to nuclear spins[18] and tends to narrow the ^{13}C NMR line shape in carbon intercalation compounds.[16] The isotropic part of the Knight shift is paramagnetic and proportional to the probability density of the conduction electrons at the nucleus $|\Psi(0)|^2$ and the density of states at the Fermi level $n(E_F)$,

$$K_{iso} = \frac{8\pi}{3}|\Psi(0)|^2 \mu_B^2 n(E_F). \tag{2}$$

K_{iso} has been estimated in pristine metallic SWNTs to be less than 10 ppm.[9,19] Since the isotropic Knight shift is proportional to $n(E_F)$, our measurements suggest an increase of $n(E_F)$ from LiC_{10} to LiC_6. However, it is not trivial to estimate $n(E_F)$ directly from the isotropic line position because of the unknown isotropic chemical shift in charged SWNTs.

In order to obtain a better estimate of $n(E_F)$, we performed ^{13}C NMR spin-lattice relaxation measurements as a function of temperature. The inset of Fig. 2 presents the magnetization recovery at room temperature for pristine and LiC_6 SWNT. For all Li intercalated samples, 96% of the ^{13}C NMR signal exhibits a single T_1 component that can be fitted by a monoexponential recovery curve after saturation.[20,21] The corresponding $1/T_1$ relaxation rates are plotted in Fig. 2. Below 50 K, the relaxation rate increases with decreasing temperature, which can be attributed to relaxation by magnetic catalyst impurities present in the sample.[8] Above 50 K, we observed a linear regime with a slope depending on the lithium intercalation level. The linear increase of the relaxation rate above 50 K is typical for a metallic Fermi liquid system. In metals, the major relaxation mechanism originates from the hyperfine coupling of conduction electron spins to the observed nuclear spins. This leads to the Korringa relation given by

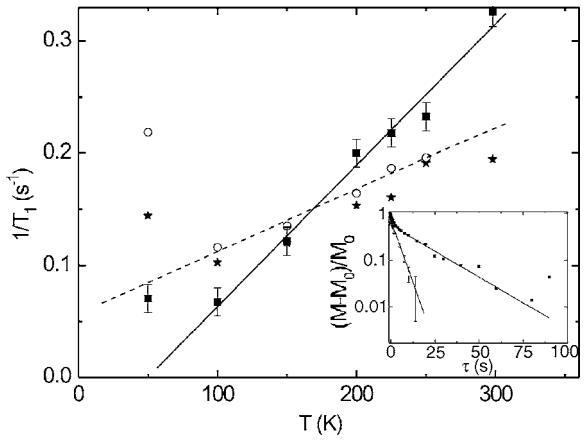

FIG. 2. Temperature-dependent ^{13}C NMR spin lattice relaxation rates (ω_0=50.3 MHz) for LiC_{10}: ⋆, LiC_7: ○, and LiC_6: ■. Inset: ^{13}C NMR magnetization recovery at room temperature for LiC_6:○ and pristine SWNT: ■ (Ref. 9).

$$\frac{1}{T_1 T} = \frac{2\pi k_B}{\hbar} A_{iso}^2 n(E_F)^2, \tag{3}$$

where A_{iso} is the isotropic hyperfine coupling constant.[18] As previously reported in pristine SWNT,[8,9,22] we assume a hyperfine coupling of $A_{iso}=8.2\times10^{-7}$ eV and fit the linear regime part of the ^{13}C NMR spin lattice relaxation. Hence, we were able to estimate the evolution of the $n(E_F)$ with the Li concentration, as reported in Table I. In agreement with line shape modifications, the maximum in $n(E_F)$ corresponds to the highest amount of intercalated Li.

We turn now to the ^7Li NMR spectra and spin lattice relaxation measurements in the temperature range from 50 to 465 K. In all the samples for all temperatures, the recovery of the magnetization follows a biexponential curve. This corresponds to two relaxation rates suggesting two inequivalent Li sites that we label α and β with $T_1^\alpha > T_1^\beta$. From the fits of the magnetization recovery, the following ratios between α and β sites can be estimated: LiC_{10} [α:70%, β:30%], LiC_7 [α:55%, β:45%], and LiC_6 [α:50%, β:50%]. Obviously, the first intercalated Li are of type α. With increasing Li concentration, a second type β is adsorbed by the SWNT host. The origin for these two inequivalent Li is unknown, but it is certainly related to the complex structure of the carbon nanotube bundles which present different adsorption sites with inequivalent environments.[23,24] In order to estimate the corresponding ^7Li NMR resonances, we investigated the line shift and linewidth during the T_1 relaxation measure-

TABLE I. Density of states at the Fermi level $n(E_F)$ for LiC_x with x=6, 7, and 10 and pristine metallic SWNT.

SWNT sample	$n(E_F)$ states/eV spin atom
LiC_6	0.032
LiC_7	0.020
LiC_{10}	0.021
Pristine metallic SWNT	0.015[9,22]

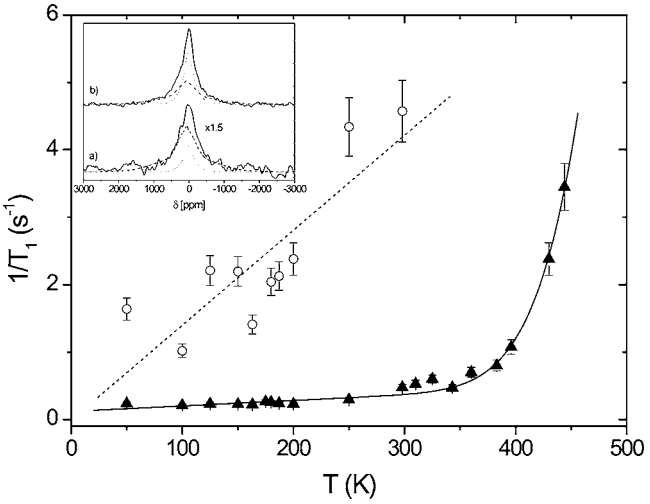

FIG. 3. Temperature-dependent ^{7}Li NMR spin lattice relaxation rate $1/T^{\alpha}$ (▲) and $1/T^{\beta}$ (○) of LiC_{10} at a Larmor frequency of $\omega_0 = 100$ MHz. The dotted line is a fit according to Eq. (4). The dashed line is a fit assuming a Korringa relaxation process. Inset: ^{7}Li NMR spectra in LiC_{10} at 50 K extracted from magnetization recovery experiments: (a) partially recovered spectrum at a short delay, 0.8 s and (b) fully relaxed spectrum at a long delay, 22 s. The ratios in (a) [α:37%, β:63%] and in (b) [α:70%, β:30%] are obtained from a deconvolution with one sharp-α (dotted line) and one broad-β (dashed line) quadrupolar shaped line as described in the text.

ments. The inset of Fig. 3 shows the spectra for LiC_{10} at 50 K for a short and a long recovery time. The best fits of the partially recovered spectrum [Fig. 3(a)] and the fully relaxed one [Fig. 3(b)] were obtained with one sharp-α and one broad-β quadrupolar shaped line-shifted to $\delta_{\alpha} \approx 10$ ppm and $\delta_{\beta} \approx 70$ ppm, respectively. The ratio of the lines was fixed according to their relaxation behavior at 50 K ($T_1^{\alpha} \approx 3.8$ s and $T_1^{\beta} \approx 0.54$ s). The corresponding quadrupolar couplings were $\Delta\omega_Q^{\alpha} \approx 2\pi \times 45$ kHz and $\Delta\omega_Q^{\beta} \approx 2\pi \times 140$ kHz with Gaussian broadenings of the central transitions $\delta\omega^{\alpha} \approx 2\pi \times 8$ kHz and $\delta\omega^{\beta} \approx 2\pi \times 19$ kHz. These line broadenings indicate a large distribution of quadrupole frequencies. The significant difference in quadrupolar interaction of the α and β line suggests a profound difference in their environment. The paramagnetic shift of the β line with respect to the α line can be interpreted as a Knight shift since the typical range of ^{7}Li chemical shifts is in the order of (+5, −10 ppm).[25] These results confirm the presence of two different sites, occupied by $Li^{+\alpha}$ cations with an ionicity close to +1 and $Li^{+\beta}$ cations with $+1 \approx \alpha > \beta$. Such Knight shifts are typical for a limited charge transfer of the 2s electron of Li stored in a dense form in nanoporosities.[26] According to recent calculations,[24] the outside-Li adsorption is energetically more favorable than the Li inside the SWNT. In particular, the curvature of the graphene layer in SWNT and the presence of high reactive dangling bonds localized on defects tend to enhance the adsorption capabilities.[2,16] Solid-state electrochemistry revealed that electrochemical Li intercalation in SWNT is only partially reversible. The authors claim that upon dedoping some Li remains trapped in the SWNT host.[27] Therefore, the quadrupolar broadened ^{7}Li NMR β line we report in the inset of Fig. 3 suggests the binding of C and $Li^{+\beta}$, uniquely observed in GIC (graphitic intercalation compounds).[28]

In order to obtain further details on the structural and electronic properties of the system, we investigated the temperature dependence of the spin lattice relaxation rate. Figure 3 presents the $1/T_1^{\alpha}$ and $1/T_1^{\beta}$ relaxation rates of the ^{7}Li NMR α and β component for LiC_{10}. $1/T_1^{\alpha}$ follows a linear increase with increasing temperature below ≈400 K and a rapid exponential increase above. According to the Korringa relation,[18] the linear relaxation regime at low temperature can be interpreted as a hyperfine coupling of the Li nuclear spins to conduction electron spins. $1/T_{1K}^{\alpha}T \approx 0.00081\ s^{-1}\ K^{-1}$ is obtained which is below the $1/T_{1K}^{G}T = 0.0016\ s^{-1}\ K^{-1}$ for a first stage Li-graphite intercalation compound LiC_6.[29] The exponential increase and deviation from Korringa's law of $1/T_1^{\alpha}$ above a temperature of ≈400 K is typical for a thermally activated BPP-type diffusion or motion modulated quadrupolar interaction. A thermally activated diffusion path of $Li^{+\alpha}$ is expected along the channels of the carbon nanotube bundles. Therefore, the relaxation of the ^{7}Li nuclei promoted by conduction electrons and fluctuation of local electric field gradients can be readily expressed according to Ref. 30 as

$$\frac{1}{T_1} = \frac{1}{T_{1B}} + \frac{1}{T_{1K}} + \frac{1}{T_{1Q}}, \quad \frac{1}{T_{1Q}} = \frac{2}{25}\Delta\omega_Q^2[J^{(1)}(\omega_0) + J^{(2)}(\omega_0)], \tag{4}$$

where $\Delta\omega_Q$ is the quadrupolar coupling constant and $J^{(1,2)} \times (\omega_0)$ are the spectral densities corresponding to a thermally activated process with

$$J^{(1)}(\omega_0) = \frac{\tau_c}{1+\omega_0^2\tau_c^2}, \quad J^{(2)}(\omega_0) = \frac{4\tau_c}{1+4\omega_0^2\tau_c^2},$$
$$\tau_c = \tau_0 \exp\left(\frac{\Delta E}{k_B T}\right). \tag{5}$$

ω_0 is the Larmor frequency, $\tau_0 \approx 10^{-12}$ s is the infinite temperature correlation time, and ΔE is the activation energy. The fit of the $1/T_1^{\alpha}$ relaxation shown in Fig. 3 results in an activation energy of $\Delta E^{\alpha} \approx 400$ meV and a relaxation background of $1/T_{1B}^{\alpha} \approx 0.12\ s^{-1}$. The quadrupolar coupling constant was estimated to $\Delta\omega_Q^{\alpha} \approx 2\pi \times 40$ kHz, which is consistent with $\Delta\omega_Q^{\alpha} \approx 2\pi \times 45$ kHz obtained from the spectra. The observed activation energy is about two times higher than reported for a first-stage Li-GIC compound LiC_6 with $\Delta E^G = 221$ meV.[31] Our activation energy is higher since bindings between Li and C and diffusion along nearly one-dimensional channels have to be overcome.

In the investigated temperature range, the $1/T_1^{\beta}$ relaxation rate in Fig. 3 follows a linear Korringa relaxation process. By applying a linear fit, a slope of $1/T_1^{\beta}T \approx 0.0135\ s^{-1}\ K^{-1}$ is obtained. This value is in between $1/T_{1K}^{G}T = 0.0016\ s^{-1}\ K^{-1}$ for a first-stage Li-graphite intercalation compound LiC_6 (Ref. 29) and $1/T_1^{M}T = 0.023\ s^{-1}\ K^{-1}$ for pure Li^0 metal.[32] These results are consistent with the strong paramagnetic Knight shift of the β component. The strong Li-C hyperfine coupling we observed suggests hybridized states between the

Li($2s$) electrons and the SWNT π electron system. This also explains well the charge-transfer limitations observed in our ^{13}C NMR measurements, which is in agreement with recent theoretical calculations.[23]

In summary, we have performed ^{13}C and ^{7}Li solid-state NMR measurements on Li intercalated SWNTs. We investigated their metallic ground state, which is tunable by the Li content, and we calculated the density of states at the Fermi level. We found the existence of two inequivalent α and β sites for Li cations and suggest binding and hybridized states between Li and C, which limits the electronic charge transfer. We also point out that Li cations show thermally activated dynamics and diffusion along the channels of the carbon nanotube bundles.

The authors thank Pierre Lauginie and Jacques Conard for helpful discussions. We acknowledge funding support by the EU project CANAPE (NMP4-CT-2004-500096).

*Author to whom all correspondence should be addressed.

[1] M. Endo, C. Kim, K. Nishimura, T. Fujio, and K. Miyashita, Carbon **38**, 183 (2000).
[2] B. Gao, A. Kleinhammes, X. P. Tang, C. Bower, L. Fleming, Y. Wu, and O. Zhou, Chem. Phys. Lett. **307**, 153 (1999).
[3] R. S. Lee, H. J. Kim, J. E. Fischer, A. Thess, and R. E. Smalley, Nature (London) **388**, 255 (1997).
[4] A. M. Rao, P. C. Eklund, S. Bandow, A. Thess, and R. E. Smalley, Nature (London) **388**, 257 (1997).
[5] A. Claye, Ph.D. thesis, University of Pennsylvania (2000).
[6] E. Hernandez, C. Goze, P. Bernier, and A. Rubio, Phys. Rev. Lett. **80**, 4502 (1998).
[7] C. Journet, W. K. Maser, P. Bernier, A. Loiseau, M. L. de la Chapelle, S. Lefrant, P. Deniard, R. Lee, and J. E. Fischer, Nature (London) **388**, 756 (1997).
[8] C. Goze-Bac, S. Latil, L. Vaccarini, P. Bernier, P. Gaveau, S. Tahir, V. Micholet, R. Aznar, A. Rubio, K. Metenier, and F. Beguin, Phys. Rev. B **63**, 100302(R) (2001).
[9] C. Goze-Bac, S. Latil, P. Lauginie, V. Jourdain, J. Conard, L. Duclaux, A. Rubio, and P. Bernier, Carbon **40**, 1825 (2002).
[10] P. Petit, E. Jouguelet, and C. Mathis, Chem. Phys. Lett. **318**, 516 (2000).
[11] N. Bendiab, E. Anglaret, J. L. Bantignies, A. Zahab, J. L. Sauvajol, P. Petit, C. Mathis, and S. Lefrant, Phys. Rev. B **64**, 245424 (2001).
[12] J. L. Sauvajol, N. Bendiab, E. Anglaret, and P. Petit, C. R. Phys. **4**, 9 (2003).
[13] L. Facchini, M. Quinton, and A. Legrand, Physica B **99**, 525 (1980).
[14] O. Tanaike and M. Inagaki, Carbon **35**, 831 (1997).
[15] M. Inagaki and O. Tanaike, Carbon **39**, 1083 (2001).
[16] P. Lauginie, Ph.D. thesis, University of Paris–Sud, Centre d'Orsay (1988).
[17] P. Petit, C. Mathis, C. Journet, and P. Bernier, Chem. Phys. Lett. **305**, 370 (1999).
[18] A. Abragam, *Principles of Nuclear Magnetism* (Oxford University Press, Oxford, 1989).
[19] S. Latil, L. Henrard, C. Goze-Bac, P. Bernier, and A. Rubio, Phys. Rev. Lett. **86**, 3160 (2001).
[20] M. Schmid, C. Goze-Bac, M. Mehring, S. Roth, and P. Bernier, in *Electronic Properties of Novel Materials, XVII International Winterschool*, edited by H. Kuzmany, K. Fink, M. Mehring, and S. Roth (World Scientific, Singapore, 2004), pp. 238 and 723.
[21] H. Shimoda, B. Gao, X. P. Tang, A. Kleinhammes, L. Fleming, Y. Wu, and O. Zhou, Phys. Rev. Lett. **88**, 015502 (2002).
[22] X. P. Tang, A. Kleinhammes, H. Shimoda, L. Fleming, K. Y. Bennoune, S. Sinha, C. Bower, O. Zhou, and Y. Wu, Science **288**, 492 (2000).
[23] J. Lu, S. Nagase, S. Zhang, and L. Peng, Phys. Rev. B **69**, 205304 (2004).
[24] Y. Liu, H. Yukawa, and M. Morinaga, Comput. Mater. Sci. **30**, 50 (2004).
[25] J. Conard and P. Lauginie, in *New Trends in Intercalation Compounds for Energy Storage*, edited byC. Julien, J. P. Pereira-Ramos, and A. Momchilov (Kluwer Academic Publishers, Dordrecht, 2002), p. 77.
[26] K. Tatsumi, J. Conard, M. Nakahara, S. Menu, P. Lauginie, Y. Sawada, and Z. Ogumi, J. Power Sources **81**, 397 (1999).
[27] A. Claye, J. E. Fischer, C. B. Huffman, A. G. Rinzler, and R. E. Smalley, J. Electrochem. Soc. **147**, 2845 (2000).
[28] J. Conard, in *New Trends in Intercalation Compounds for Energy Storage*, edited by C. Julien, J. P. Pereira-Ramos, and A. Momchilov (Kluwer Academic Publishers, Dordrecht, 2002), p. 63.
[29] H. Estrade, J. Conard, P. Lauginie, P. Heitjans, F. Fujara, W. Buttler, G. Kiese, H. Ackermann, and D. Guerard, Physica B **99**, 531 (1980).
[30] M. Mehring and A. Weberruss, *Object-Oriented Magnetic Resonance* (Academic Press, San Diego, 2001).
[31] P. Yu, B. N. Popov, J. A. Ritter, and R. E. White, J. Electrochem. Soc. **146**, 8 (1999).
[32] A. G. Anderson and A. G. Redfield, Phys. Rev. **116**, 583 (1959).